Stokes' dream: Measurement of fluid viscosity from the attenuation of capillary waves

F. Behroozi,[a] J. Smith,[b] and W. Even[c]
Department of Physics, University of Northern Iowa, Cedar Falls, Iowa 50614

(Received 21 March 2010; accepted 6 July 2010)

The determination of viscosity from the attenuation of capillary waves was first suggested by Stokes more than a century ago. At the time, it was not practical to measure the attenuation of surface waves with the requisite precision to render the method useful. We describe a noncontact method for measuring the wavelength and amplitude of single-frequency capillary waves to obtain reliable values of the surface tension and viscosity. The attenuation data for several glycerin-water mixtures are used to obtain the viscosity as a function of glycerin concentration. For a wide range of viscosity, the method yields results that are in good agreement with the most reliable published data. © *2010 American Association of Physics Teachers.*
[DOI: 10.1119/1.3467887]

I. INTRODUCTION

Surface waves on fluids with wavelengths ranging from a few millimeters down to a fraction of a micrometer are known as capillary waves.[1] More than a century ago, Stokes pointed out that the attenuation of capillary waves could be exploited to measure fluid viscosity and worked out the relation between viscosity and wave attenuation.[2,3] At the time, no practical technique was available to measure the attenuation of single frequency surface waves with the requisite precision to render the method useful for routine measurements of viscosity.

The standard method for measuring viscosity was invented by Poiseuille who devised the first flow viscometer.[4] A flow viscometer exploits the relation between the fluid viscosity and its flow rate through a horizontal capillary tube under a given hydrostatic pressure. Others, including Maxwell, devised alternative viscometers (Couette, oscillating disk, and cone and plate viscometers),[5–7] which measure viscosity by exploiting the resistance experienced by an object in contact with and in relative motion to the fluid.

Advances in surface light scattering had led to renewed attention to Stokes' idea,[8–14] particularly because it offers the possibility of measuring viscosity noninvasively. The experimental method of choice in most recent studies has been photon correlation spectroscopy, where the line broadening of scattered laser light from thermally excited capillary waves is analyzed to extract dispersion and attenuation data.[15–17]

Unfortunately, for thermally exited waves, we are limited to the very short wavelength regime of submicrometer waves.[18] This limitation is problematic in that a significant reduction in surface energy of liquid interfaces is observed at short length scales.[19] Because surface tension governs the dispersion of capillary waves, attenuation data are greatly affected by the reduction of surface tension at the very short wavelengths associated with thermally excited waves. It appears that light scattering data from thermal capillary waves do not provide reliable rheological parameters for typical polymers or fatty acids.[20] Nevertheless, interest in the technique remains high, principally because light scattering and correlation spectroscopy are well-developed areas of optics[21] and partly because the technique is well adapted for use with x-rays.[22]

The propagation and attenuation of capillary waves are governed respectively by surface tension and viscosity, while gravity plays a minor role.[23] Therefore, the dispersion and attenuation of capillary waves may be used to obtain the surface tension and viscosity of fluids.[24,25] We describe a noncontact method for the precision measurement of the dispersion and attenuation of capillary waves on fluids. The dispersion data give the surface tension,[26,27] and the attenuation data yield the viscosity.[28]

We use a novel miniature laser interferometer[29] to obtain the wave profile with a resolution of about 5 nm. The attenuation data for several glycerin-water mixtures with glycerin concentrations of up to 70% are used to obtain the viscosity of the mixtures. The results are in good agreement with the most reliable published data.[30]

II. EXPERIMENTAL TECHNIQUE

The experimental technique has been described in Refs. 31 and 32. Here we present a summary and include the most recent improvements in the system.

A Teflon trough (6×46 cm^2 with a depth of 1 cm) is used to contain the fluid. Thermoelectric cells underneath the trough regulate the temperature. The system rests on a vibration free isolation table and is housed in an enclosure to minimize air currents.

Single frequency capillary waves are generated electronically by placing a metallic blade a few tenths of a millimeter above the fluid surface (see Fig. 1). A dc-biased sinusoidal voltage of a few hundred volts at a selected frequency is applied between the blade and the fluid. For polar fluids such as water or water-based binary mixtures, the ac component of the electric field under the blade generates two capillary wave trains that recede from the blade on each side. A typical wavelength is about 1 mm, and the wave amplitude is usually less than 1 μm. Because the wavelength of the capillary waves is a fraction of the depth of the trough, the deep fluid formalism applies.

Figure 1 shows one wave-generating blade and a fiber probe above the capillary wave. The fiber-optic probe is mounted on an electronic micrometer, which records the probe position with an accuracy of about 1 μm. In this schematic, the wave amplitude has been exaggerated for clarity. d_0 is the distance from the tip of the probe to the equilibrium surface. When a wave is present, Δ represents the roundtrip distance from the tip of the probe to the fluid surface.

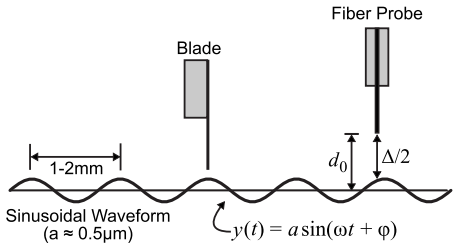

Fig. 1. Schematic of a fiber probe and wave-generating blade. The wave amplitude has been exaggerated for clarity.

The amplitude of capillary waves is detected by using a fiber-optic system, which functions as a miniature laser interferometer. The system consists of a single mode optical fiber, one end of which is positioned a short distance above the fluid surface (see Fig. 1). Laser light, traveling through the optical fiber, is partially reflected from the cleaved tip of the fiber and again from the fluid surface. The two reflected beams travel back through the same fiber and generate an interference signal at the detector. As the fluid level under the probe changes due to the wave motion, the gap between the fiber tip and the fluid surface changes, causing a periodic change in the path difference Δ. Thus, the number of fringes in the periodic interference signal gives an accurate measure of the wave amplitude.

The interference signal is measured by photodetectors, and is amplified and digitized for later analysis. In Fig. 2, the raw interference signal for a half period is shown at the top of the frame. The solid curve is the fit, which replicates the trace faithfully. The dashed curve gives the vertical displacement of the surface wave under the probe as a function of time.

Because there is a one to one correspondence between the surface wave amplitude and the resulting interference pattern, the profile of the surface wave can be recovered by counting the number of fringes in the interference pattern. As discussed in Ref. 28, the number of fringes in the interference pattern is directly proportional to the vertical displacement of the surface wave under the probe. For the pattern shown in Fig. 5, the number of fringes is 6.78, and the amplitude of the wave is 1.07 μm.

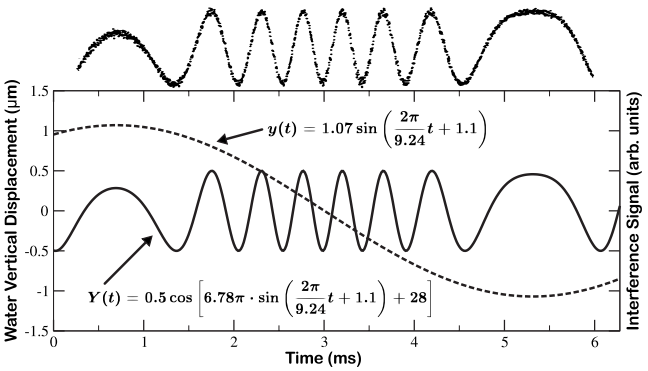

Fig. 2. The interference signal for one half-wavelength. The raw interference signal for the half period is shown at the top of the frame. The solid curve is the fit, and the dashed curve gives the vertical displacement. The right scale is for the interference signal, and the left scale is for the wave amplitude.

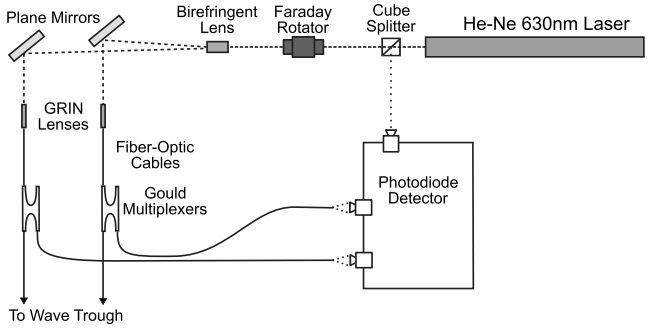

Fig. 3. Schematic of the optical and electronic detection system.

III. DETERMINATION OF THE WAVE AMPLITUDE

The schematic of the optoelectronic system is shown in Fig. 3. Part of the beam from the He–Ne laser is split by the cube splitter and used as a reference signal at the detector to compensate for any laser output fluctuations. The main beam passes through a birefringent lens and is split into two equal beams for use in the two fiber-optic probes. The Gould multiplexer is essential in routing the interference signal to the detector and preventing reflected signals from getting back to the laser. The Faraday rotator further isolates and protects the laser cavity from "seeing" any reflected signal.

To determine the wave amplitude of a traveling wave from the interference record, we assume that the vertical oscillation of the fluid surface under the probe is given by

$$y(t) = a\,\sin(\omega t + \beta), \tag{1}$$

where a is the wave amplitude, ω is the angular frequency, t is the time, and β is a phase that depends only on the position of the probe relative to the blade. Because d_0 is the air gap between the probe and the equilibrium surface of the fluid, the path difference between the two reflected beams is given by (see Fig. 1)

$$\Delta = 2[d_0 - a\,\sin(\omega t + \beta)]. \tag{2}$$

Consequently, the phase difference between the two reflected beams is $[(2\pi\Delta/\lambda_l) + \pi]$, where λ_l is the wavelength of the laser light; π is added to the phase to account for the fact that the light beam reflecting from the fluid surface suffers a phase shift of π radians. Therefore, the ac component of the resulting interference pattern is given by

$$Y(t) = A\,\cos[(2\pi\Delta/\lambda_l) + \pi], \tag{3}$$

where A is the amplitude of the interference signal. If Eq. (2) is substituted in Eq. (3), the result is

$$Y(t) = A\,\cos[b\,\sin(\omega t/\beta) - \phi], \tag{4}$$

where the parameters b and ϕ are defined as

$$b = 4\pi a/\lambda_l, \tag{5}$$

$$\phi = (\pi + 4\pi d_o/\lambda_l). \tag{6}$$

Equation (4) is the functional form of the interference signal. The number of interference fringes is proportional to the wave amplitude and is given by

$$\text{number of fringes} = 4a/\lambda_l = b/\pi. \tag{7}$$

The wave amplitude is equal to the wavelength of light multiplied by one-fourth of the number of fringes,

$$a = b\lambda_l/4\pi. \tag{8}$$

In light of Eq. (8), it is necessary only to extract the parameter b by fitting the analytical expression in Eq. (4) to the interference data to obtain the amplitude of the capillary wave. To do so, the interference signal is digitized and used as input in a multivariable fit routine, which adjusts the four parameters of Eq. (4) until a good fit is achieved. Of the four parameters in Eq. (4), A and β are readily available from the raw data, and thus the fit reduces to a search in the two-parameter space of b and ϕ. The fit is easily accomplished by an initial estimate of b obtained by counting the number of fringes and examining the asymmetry in the interference pattern to estimate ϕ. The fit is then refined incrementally by minimizing the difference between the fit and the normalized data. It is possible to use Bessel functions to deconvolute the interference data analytically to obtain the parameters b and ϕ in terms of the moments of the data.[33]

The dissipation of wave energy due to viscosity manifests itself in the attenuation of the amplitude as the wave travels along the surface away from the source. The wave amplitude decays exponentially as the waves travel a distance x,

$$a = a_0 e^{-\alpha x}, \tag{9}$$

where a_0 is the reference amplitude at $x=0$ and α is the attenuation coefficient. As described in Ref. 25, the attenuation coefficient is related to the fluid viscosity μ by the relation

$$\alpha = 2k^2\mu/\rho v_g, \tag{10}$$

where $k=2\pi/\lambda$ is the wave number, λ is the capillary wavelength, and v_g is the group velocity of capillary waves given by[24]

$$v_g = (g + 3\sigma k^2/\rho)/2(kg + \sigma k^3/\rho)^{1/2}. \tag{11}$$

If Eq. (11) is used in Eq. (10), we obtain the viscosity in terms of four measurable quantities, namely, k, σ, ρ, and α. Therefore we have

$$\mu = (\alpha\rho/2k^2)(g + 3\sigma k^2/\rho)/2(kg + \sigma k^3/\rho)^{1/2}. \tag{12}$$

The attenuation coefficient α is obtained from a plot of the wave amplitude as a function of distance from a reference point. Because the wave amplitude decays exponentially with distance, it is sufficient to determine the wave amplitude at two positions, x_1 and x_2, along the direction of propagation, and α is given by

$$\alpha = \ln(a_1/a_2)/(x_2 - x_1). \tag{13}$$

The wavelength λ and surface tension σ are determined as follows. First, a standing wave is established on the fluid surface by use of two blades, separated by a few centimeters, which generate waves of the same phase, amplitude, and frequency. Because each blade sends a wave train toward the other, a standing capillary wave is established on the surface between the two blades. If the distance between the two blades is chosen to be a half odd-integer wavelength, the two wave trains interfere destructively on the outer sides of the blades. This judicious choice of the blades' separation produces a region of standing waves between the blades, while the surface outside the blades remains calm. This arrangement renders moot the possible interference of reflected waves from far boundaries of the trough at low frequencies.

The measurement of the distance between several nodes of the standing capillary waves yields the wavelength for a given frequency. In our setup, the fiber-optic probe is attached to a micropositioner, which is equipped with a digital micrometer. This setup enables us to measure the wavelength of the standing capillary waves to within a micrometer.

At frequencies greater than 500 Hz or when the fluid is several times more viscous than water, the attenuation is too strong to establish standing waves. In this case, only one blade is used to generate a wave train. A probe is then used to scan the fluid surface starting from a point as close to the exciting blade as possible and moving away. The interference pattern on the digital scope shifts through a complete period as the probe on the surface travels through a wavelength. In this way the probe may be moved through several wavelengths as the interference pattern on the scope shifts through the same number of periods. The micrometer reading gives an accurate measure of the wavelength.

The experimental dispersion data yield the surface tension when the data are fitted to the dispersion relation for capillary waves. The full dispersion relation for capillary-gravity waves[34] may be written as

$$(i\omega + 2\mu k^2/\rho)^2 + gk + \sigma k^3/\rho = (4\mu^2 k^3/\rho^2)(k^2 + i\omega\rho/\mu)^{1/2}, \tag{14}$$

where ω is the angular velocity and g is the acceleration of gravity. As expected, Eq. (14) reduces to the familiar dispersion relation when $\mu=0$,

$$\omega^2 = kg + k^3\sigma/\rho. \tag{15}$$

If viscosity is not neglected, Eq. (14) reduces in the first approximation to

$$\omega^2 = gk + k^3[\sigma/\rho - (8\mu^3\omega/\rho^3)^{1/2} + 4k\mu^2/\rho^2]. \tag{16}$$

Ordinarily, the second and third terms in the brackets involving μ are small relative to the first term and tend to cancel one another. For a 40% glycerin-water mixture at 100 Hz, the contribution from the second and third terms is about 0.2% of the first term.

We may recast Eq. (16) in the more familiar form,

$$\omega^2 = kg + (\sigma_{\text{eff}}/\rho)k^3, \tag{17}$$

where

$$\sigma_{\text{eff}} \equiv \sigma - (8\mu^3\omega/\rho)^{1/2} + 4k\mu^2/\rho. \tag{18}$$

In practice, we fit the experimental dispersion data to Eq. (17) to obtain σ_{eff} for use in Eq. (12).

IV. RESULTS AND DISCUSSION

Figure 4 is a typical plot of the phase velocity versus wavelength for a glycerin-water mixture containing 20% glycerin at a temperature of 25 °C. Each data point is obtained by measuring the wavelength of a standing wave established between the two blades at a given frequency. The value of σ_{eff}/ρ is obtained from this plot by fitting the data to Eq. (17).

To obtain the attenuation coefficient of the capillary waves, only one blade is used to generate a traveling surface wave train at a particular frequency. Two fiber probes are employed for this measurement. One probe is held stationary at a reference point several wavelengths away from the generating blade, while the other probe is moved to points pro-

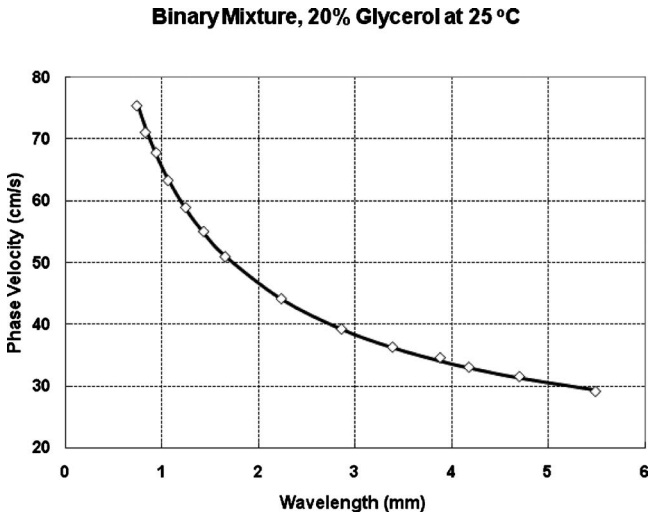

Fig. 4. Phase velocity versus wavelength for a binary mixture with 20% glycerin and temperature of 25 °C.

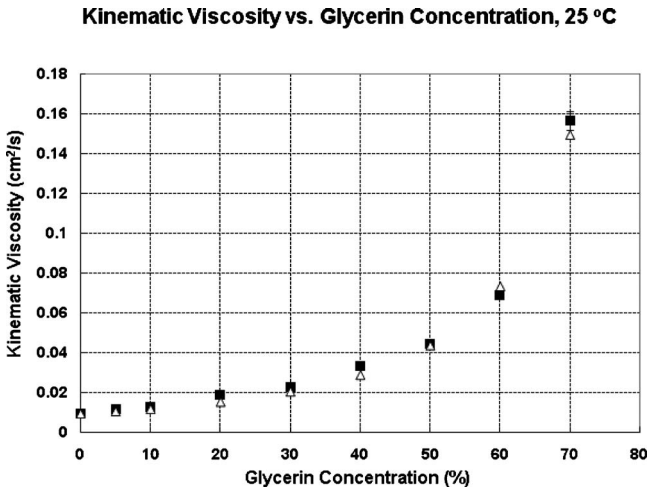

Fig. 6. Kinematic viscosity versus glycerin concentration for several binary mixtures at 25 °C. The solid squares are the measured data; the open triangles are data from Ref. 30. The viscosity data are very sensitive to temperature variations, which explains the small differences between the two data sets.

gressively farther from the reference. The ratio of the two wave amplitudes gives a normalized measure of the wave attenuation as a function of distance. This method automatically corrects for any changes in the interference signal caused by a change in the fluid level under the exciting blade due to evaporation.

Figure 5 is a typical plot of the wave amplitude as a function of the distance. The binary mixture is the same one used to obtain the dispersion data in Fig. 4. The wave frequency is 151 Hz and the temperature is 25 °C. The attenuation data give the normalized amplitude of the wave as it moves away from the source. The attenuation coefficient α is obtained from an exponential fit to the data points as shown by the solid line.

In practice, α is obtained by placing the two probes at positions x_1 and x_2. The ratio of the wave amplitudes under the two probes, a_1/a_2, gives α from Eq. (13).

The attenuation coefficient α is a function of wavelength and hence frequency. As seen in Eq. (10), α is proportional to k^2. However, the viscosity μ as given by Eq. (12) is frequency independent because α appears in Eq. (12) in the form α/k^2. This observation allows us to obtain the attenuation coefficient at any convenient frequency for use in Eq. (12). In practice, we measure α for a mixture at several frequencies and calculate the viscosity to provide a good error estimate.

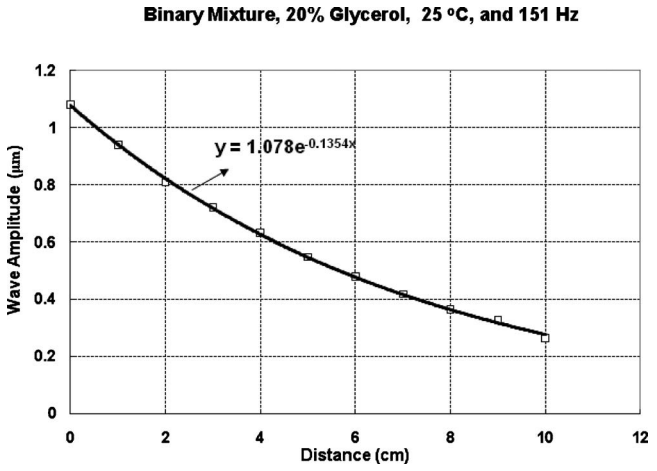

Fig. 5. Wave amplitude versus distance for a binary mixture with 20% glycerin at a frequency of 151 Hz and temperature of 25 °C. The solid line is an exponential fit to the data.

Figure 6 gives the kinematic viscosity of several glycerin-water binary mixtures as a function of the glycerin concentration. The solid circles represent our measurements, and the open triangles give the recent data of Kumar and Shankar[30] obtained by traditional flow viscometry. The two sets of data are in good agreement. The small discrepancies are due to temperature fluctuations during taking data in our system.

The measurement of the viscosity from the attenuation of capillary waves is possible because the new interferometer gives the wave amplitude of surface waves with a resolution of about 1 μm or about two orders of magnitude better than the resolution of a typical optical microscope. Our technique offers a noncontact method to determine the dispersion and attenuation data of capillary waves on polar fluids. Dispersion data may be used to obtain an accurate value of the surface tension, while the attenuation data give the viscosity. The new results compare favorably with the most reliable data obtained by traditional flow viscometry. We have checked our results against viscosity data obtained by using the same binary mixtures in a flow viscometer. When the fluid temperature is well controlled, the results are identical to those obtained from the attenuation data.

As a viscometer, the system is sensitive enough to measure small changes in the viscosity of pure water as a function of temperature. Because water has a very small viscosity, measuring the temperature dependence of its viscosity as the temperature changes by a few degrees constitutes a severe test of the sensitivity of our method. The excellent results presented in Ref. 28 show that the new method provides an alternative to flow viscometry. We have shown that it may also be used on fluids with a wide range of viscosities. The noncontact nature of the method provides another advantage by eliminating the possibility of contamination of the fluid.

ACKNOWLEDGMENTS

Financial support from the Carver Trust, UNI Applied Technology Fund, and the Iowa Space Grant Consortium is gratefully acknowledged.

[a]Electronic mail: behroozi@uni.edu
[b]Present address: Sandia National Laboratories, Box 5800, Albuquerque, NM 87185.
[c]Present address: Department of Physics, Louisiana State University, Baton Rouge, Louisiana 70803.

[1]E. H. Lucassen-Reynders and J. Lucassen, "Properties of capillary waves," Adv. Colloid Interface Sci. **2**, 347–395 (1970).
[2]G. G. Stokes, *Mathematical and Physical Papers*, Vol. 3 (Cambridge U. P., Cambridge, 1901), pp. 1–141.
[3]M. J. Lighthill, *Waves in Fluids* (Cambridge U. P., Cambridge, 1978), p. 234.
[4]T. E. Faber, *Fluid Dynamics for Physicists* (Cambridge U. P., Cambridge, 1995), pp. 29–30.
[5]T. E. Faber, *Fluid Dynamics for Physicists* (Cambridge U. P., Cambridge, 1995), pp. 222–224.
[6]R. S. Higginbotham, "A cone and plate viscometer," J. Sci. Instrum. **27**, 139–141 (1950).
[7]R. Dipippo, J. Kestin, and J. H. Whitelaw, "A high-temperature oscillating-disk viscometer," Physica (Amsterdam), **32**(11–12), 2064–2080 (1966).
[8]J. S. Huang and W. W. Webb, "Viscous damping of thermal excitations on the interface of critical fluid mixtures," Phys. Rev. Lett. **23**, 160–163 (1969).
[9]Ka Yee Lee, Tom Chou, Doo Soo Chung, and Eric Mazur, "Direct measurement of spatial damping of capillary waves at liquid-vapor interfaces," J. Phys. Chem. **97**, 12876–12878 (1993).
[10]Andrew Belmonte and Jean-Marc Flesselles, "Experimental determination of the dispersion relation for spiral waves," Phys. Rev. Lett. **77**, 1174–1177 (1996).
[11]Carlos Martel and Edgar Knobloch, "Damping of nearly inviscid water waves," Phys. Rev. E **56**, 5544–5548 (1997).
[12]U-Ser Jeng, Levon Esibov, Lowel Crow, and Albert Steyerl, "Viscosity effect on capillary waves at liquid interfaces," J. Phys.: Condens. Matter **10**, 4955–4962 (1998).
[13]David R. Howell, Wook Hwang Ben Buhrow, and Michael F. Schatz, "Measurement of surface-wave damping in a container," Phys. Fluids **12**, 322–326 (2000).
[14]P. Cicuta and I. Hopkinson, "Dynamic light scattering from colloidal fractal monolayers," Phys. Rev. E **65**, 041404-1–5 (2002).
[15]R. H. Katyl and U. Ingard, "Line broadening of light scattered from liquid surface," Phys. Rev. Lett. **19**, 64–66 (1967).
[16]J. C. Earnshaw, "Surface light scattering: A methodological review," Appl. Opt. **36**, 7583–92 (1997).
[17]D. M. Buzza, "General theory for capillary waves and surface light scattering," Langmuir **18**, 8418–35 (2002).
[18]J. C. Earnshaw and C. J. Hughes, "High frequency capillary waves on the clean surface of water," Langmuir **7**, 2419–2421 (1991).
[19]C. Fradin, A. Braslau, D. Luzet, D. Smilgies, M. Alba, N. Boudet, K. Mecke and J. Daillant, "Reduction in surface energy of liquid interfaces at short length scales," Nature (London) **403**, 871–874 (2000).
[20]P. Cicuta and I. Hopkinson, "Recent development of surface light scattering as a tool for optical-rheology of polymer monolayers," Colloids Surf., A **233**, 97–107 (2004).
[21]D. Langevin, *Light Scattering by Liquid Surfaces and Complementary Techniques* (Dekker, New York, 1992).
[22]A. Madsen, T. Seydel, M. Sprung, C. Gutt, M. Tolan, and G. Grubel, "Capillary waves at the transition from propagating to overdamped behavior," Phys. Rev. Lett. **92**, 096104-1–4 (2004).
[23]F. Behroozi and N. Podolefsky, "Capillary-gravity waves and the Navier-Stokes equation," Eur. J. Phys. **22**, 587–593 (2001).
[24]F. Behroozi and N. Podolefsky, "Dispersion of capillary-gravity waves: A derivation based on conservation of energy," Eur. J. Phys. **22**, 225–231 (2001).
[25]F. Behroozi, "Fluid viscosity and the attenuation of surface waves: A derivation based on conservation of energy," Eur. J. Phys. **25**, 115–122 (2004).
[26]F. Behroozi and A. Perkins, "Direct measurement of the dispersion relation of capillary waves by laser interferometry," Am. J. Phys. **74**, 957–961 (2006).
[27]F. Zhu, R. Miao, C. Xu, and Z. Cao, "Measurement of the dispersion relation of capillary waves by laser diffraction," Am. J. Phys. **75**, 896–898 (2007).
[28]F. Behroozi, B. Lambert, and B. Buhrow, "Direct measurement of the attenuation of capillary waves by laser interferometry: Non-contact determination of viscosity," Appl. Phys. Lett. **78**, 2399–2402 (2001).
[29]F. Behroozi, "Apparatus and method for measurement of fluid viscosity," U.S. Patent 6,563,588 B2, May 13, 2003.
[30]P. N. Shankar and M. Kumar, "The kinematic viscosity of glycerol-water mixtures," Proc. R. Soc. London **444**, 573–581 (1994).
[31]F. Behroozi, B. Lambert, and B. Buhrow, "Noninvasive measurement of viscosity from damping of capillary waves," ISA Trans. **42**, 3–8 (2003).
[32]P. S. Behroozi, K. Cordray, W. Griffin, and F. Behroozi, "The calming effect of oil on water," Am. J. Phys. **75**, 407–414 (2007).
[33]F. Behroozi and P. S. Behroozi, "Efficient deconvolution of noisy periodic interference signals," J. Opt. Soc. Am. A **23**, 902–905 (2006).
[34]H. Lamb, *Hydrodynamics*, 6th ed. (Dover, New York, 1945), p. 627.